



**HAL**  
open science

## EIMS Fragmentation and MRM quantification of ferulic and p-coumaric acid TMS derivatives in deposited atmospheric particles.

Jean-Francois Rontani, Bruno Charrière, Christophe Menitti, Dominique Aubert, Frederic Vaultier, Claude Aubert

► **To cite this version:**

Jean-Francois Rontani, Bruno Charrière, Christophe Menitti, Dominique Aubert, Frederic Vaultier, et al.. EIMS Fragmentation and MRM quantification of ferulic and p-coumaric acid TMS derivatives in deposited atmospheric particles.. *Rapid Communications in Mass Spectrometry*, 2022, 36 (11), pp.e9287. 10.1002/rcm.9287 . hal-03810268

**HAL Id: hal-03810268**

**<https://hal.science/hal-03810268>**

Submitted on 11 Oct 2022

**HAL** is a multi-disciplinary open access archive for the deposit and dissemination of scientific research documents, whether they are published or not. The documents may come from teaching and research institutions in France or abroad, or from public or private research centers.

L'archive ouverte pluridisciplinaire **HAL**, est destinée au dépôt et à la diffusion de documents scientifiques de niveau recherche, publiés ou non, émanant des établissements d'enseignement et de recherche français ou étrangers, des laboratoires publics ou privés.



**EIMS Fragmentation and MRM quantification of ferulic and p-coumaric acid TMS derivatives in deposited atmospheric particles**

Journal:	<i>Rapid Communications in Mass Spectrometry</i>
Manuscript ID	RCM-21-0268
Wiley - Manuscript type:	Research Article
Date Submitted by the Author:	10-Nov-2021
Complete List of Authors:	RONTANI, Jean-François; Mediterranean Institute of Oceanography, Aix-Marseille University Charrière, Bruno; Centre de formation et de recherche sur l'environnement marin Aubert, Dominique; Centre de formation et de recherche sur l'environnement marin Menniti, Christophe; Centre de Formation et de Recherche sur l'Environnement Marin AUBERT, Claude; Laboratoire de Pharmacocinétique et Toxicocinétique (EA 3286)
Keywords:	P-coumaric acid, ferulic acid, Mass fragmentation, MRM quantification, Atmospheric particles
Abstract:	Ferulic and p-coumaric acids are important biological and structural components of plant cell walls and possess antioxidant and antimicrobial properties. These phenolic acids are widespread in environmental samples. However, when they are present at very low concentrations or in very complex lipid extracts, their identification and quantification can be challenging. The EIMS fragmentation pathways of ferulic and p-coumaric acid TMS derivatives were investigated. These pathways were deduced by (i) low-energy CID-GC/MS/MS, (ii) accurate mass measurement, and (iii) <sup>13</sup> C labelling. These compounds were then characterized and quantified in MRM mode in total lipid extracts of deposited atmospheric particles using highly specific transitions based on the main fragmentation pathways elucidated.

SCHOLARONE™  
Manuscripts

1  
2  
3  
4 1  
5  
6  
7  
8 2  
9  
10  
11 3 **EIMS Fragmentation and MRM quantification of**  
12  
13  
14 4 **ferulic and *p*-coumaric acid TMS derivatives in**  
15  
16  
17 5 **deposited atmospheric particles**  
18  
19  
20 6  
21  
22 7  
23  
24 8  
25 9  
26 9  
27  
28  
29 10  
30  
31 11  
32

33 12 Jean-François Rontani<sup>1\*</sup>, Bruno Charrière<sup>2</sup>, Dominique Aubert<sup>2</sup>,  
34 13 Christophe Menniti<sup>2</sup>, Frédéric Vaultier<sup>1</sup> and Claude Aubert<sup>3</sup>  
35 14  
36 15  
37 16  
38 17  
39 18  
40 19  
41 19  
42  
43 20  
44  
45 21  
46  
47 22  
48  
49 23  
50  
51 24  
52  
53 25  
54  
55 26  
56  
57

33 12 <sup>1</sup> Aix Marseille Univ, Université de Toulon, CNRS, IRD, MIO UM 110, Marseille, France,  
34 13 13288, Marseille, France.

36 15 <sup>2</sup> Centre de Formation et de Recherche sur les Environnements Méditerranéens (CEFREM,  
37 16 UMR CNRS UPVD 5110), 52 Avenue Paul Alduy, 66860 Perpignan Cedex, France  
38 17

40 18 <sup>3</sup> Laboratoire de Pharmacocinétique et Toxicocinétique (EA 3286), Faculté de Pharmacie,  
41 19 13385 Marseille, France.  
42  
43 20  
44  
45 21  
46  
47 22  
48  
49 23  
50  
51 24  
52  
53 25  
54  
55 26  
56  
57

58 27 \* Corresponding author. Tel.: +33-4-86-09-06-02; fax: +33-4-91-82-96-41. E-mail address:  
59 28 jean-francois.rontani@mio.osupytheas.fr (J.-F. Rontani).

1  
2  
3 29  
4  
56 30 **RATIONALE**

7  
8 31 Ferulic and *p*-coumaric acids are important biological and structural components of plant cell  
9  
10 32 walls and possess antioxidant and antimicrobial properties. These phenolic acids are  
11  
12 33 widespread in environmental samples. However, when they are present at very low  
13  
14 34 concentrations or in very complex lipid extracts, their identification and quantification can be  
15  
16 35 challenging.

17  
18  
19 36 **METHODS**

20  
21  
22 37 The EIMS fragmentation pathways of ferulic and *p*-coumaric acid TMS derivatives were  
23  
24 38 investigated. These pathways were deduced by (i) low-energy CID-GC/MS/MS, (ii) accurate  
25  
26 39 mass measurement, and (iii) <sup>13</sup>C labelling. These compounds were then characterized and  
27  
28 40 quantified in MRM mode in total lipid extracts of deposited atmospheric particles using highly  
29  
30 41 specific transitions based on the main fragmentation pathways elucidated.

31  
32  
33 42 **RESULTS**

34  
35 43 CID-MS/MS analyses, accurate mass measurement and <sup>13</sup>C labelling enabled us to elucidate  
36  
37 44 EIMS fragmentations of ferulic and *p*-coumaric acid TMS derivatives. Some specific  
38  
39 45 fragmentations proved useful for subsequent characterization and quantification of these  
40  
41 46 compounds. As an application of some of the described fragmentations, trace amounts of these  
42  
43 47 phenolic acids were characterized and quantified in MRM mode in wet- and dry-deposited  
44  
45 48 atmospheric particles containing low proportions of organic matter.

46  
47  
48  
49 49 **CONCLUSIONS**

50  
51 50 EIMS fragmentations of ferulic and *p*-coumaric acid TMS derivatives exhibit specific fragment  
52  
53 51 ions that can be very useful for the quantification of trace amounts of both phenolic acids in  
54  
55 52 environmental samples.

56  
57  
58  
59 53  
60

1  
2  
3 54 **RUNNING TITLE:** Mass fragmentation of *p*-hydroxycinnamic acids  
4  
5  
6 55

7  
8 56 **KEYWORDS:** EIMS fragmentation; Ferulic acid; *p*-Coumaric acid; TMS derivatives;  
9

10 57 Deposited atmospheric particles.  
11  
12 58  
13  
14  
15  
16  
17  
18  
19  
20  
21  
22  
23  
24  
25  
26  
27  
28  
29  
30  
31  
32  
33  
34  
35  
36  
37  
38  
39  
40  
41  
42  
43  
44  
45  
46  
47  
48  
49  
50  
51  
52  
53  
54  
55  
56  
57  
58  
59  
60

For Peer Review

## 59 1 INTRODUCTION

60 Ferulic (3-(4-hydroxy-3-methoxyphenyl)prop-2-enoic) and *p*-coumaric (3-(4-hydroxyphenyl)-  
61 prop-2-enoic) acids, mostly in their *trans* isomeric forms,<sup>[1]</sup> are common constituents of the cell  
62 walls of several plant families,<sup>[2-4]</sup> where they occur either free or bound to cell wall  
63 components.<sup>[5]</sup> The binding involves ether linkages with lignin and ester linkages with structural  
64 macromolecules such as polysaccharides and proteins.<sup>[4,6]</sup> *p*-Coumaric acid is principally  
65 esterified on lignin units, and ferulic acid is both etherified to lignin and esterified to  
66 hemicelluloses.<sup>[7]</sup>

67 These secondary products of the plant metabolism have antioxidant, anti-inflammatory,  
68 anti-microbial, and anti-ageing properties.<sup>[8]</sup> They owe their highly efficient antioxidant activity  
69 to their ability to scavenge free radicals, donate hydrogen atoms, electrons, or chelate metal  
70 cations.<sup>[9]</sup> Various and informative proportions of *p*-coumaric and ferulic acids are present in  
71 pollen and spores, where they play a protective role against UV, microbial and physical  
72 damage.<sup>[10]</sup> These phenolic acids can thus be useful tools to trace organic matter origin in  
73 atmospheric particle samples.

74 The analytical techniques commonly used to quantify phenolic acids are high  
75 performance liquid chromatography (HPLC) and gas chromatography (GC), alone or in tandem  
76 with mass spectrometry (MS).<sup>[11]</sup> Despite an abundant literature,<sup>[4,12,13]</sup> quantification of these  
77 compounds in complex lipid extracts of plants or in samples containing very low amounts of  
78 organic matter remains a challenge. There is thus a real need to develop methods for the  
79 quantification of trace amounts of specific phenolic compounds in environmental samples.

80 Its high sensitivity and resolving power make GC/EIMS/MS a technique particularly  
81 well-suited to the unambiguous detection of phenolic compounds in environmental samples.  
82 Here, we set out (i) to elucidate the electron ionization (EI) fragmentation pathways of  
83 trimethylsilyl (TMS) derivatives of ferulic and *p*-coumaric acids and (ii) to quantify these

1  
2  
3 84 compounds in different samples of deposited atmospheric particles in multiple reaction  
4  
5 85 monitoring (MRM) mode using highly specific transitions based on the main fragmentation  
6  
7 86 pathways elucidated.  
8  
9

10 87

## 11 12 88 **2 EXPERIMENTAL**

13  
14  
15 89

### 16 17 90 **2.1 Chemicals**

18  
19  
20 91 *N,O*-Bis(trimethylsilyl)trifluoroacetamide (BSTFA) and unlabelled *trans*-ferulic and *trans-p*-  
21  
22 92 coumaric acids were purchased from Sigma-Aldrich (Lyon, France). *cis*-Ferulic and *cis-p*-  
23  
24 93 coumaric acids were produced by sunlight irradiation of the *trans* isomers in methanol.<sup>[14]</sup> Fully  
25  
26 94 <sup>13</sup>C-labelled *trans*-ferulic and *trans-p*-coumaric acids were isolated (97% <sup>13</sup>C) from leaves of  
27  
28 95 *Avena sativa* obtained from IsoLife (Wageningen, The Netherlands). This isolation involved  
29  
30 96 alkaline hydrolysis of leaf debris and purification of the resulting total lipid extract by  
31  
32 97 preparative thin layer chromatography (TLC) on silica gel K6 plates (Whatman, Maidstone,  
33  
34 98 UK) after elution with CHCl<sub>3</sub>/CH<sub>3</sub>OH/HCOOH (85:15:1, v/v/v).  
35  
36  
37  
38  
39

40 99

### 41 100 **2.2 Sampling and treatment of deposited atmospheric particle samples**

42  
43 101 Wet- and dry-deposited atmospheric samples were collected at Cap Béar close to the  
44  
45 102 Mediterranean Sea (42°30'54.82" N; 3°7'21.06" E) using an MTX ARS 1000 autosampler  
46  
47 103 (MTX-Italia SPA, Modena, Italia) equipped with a rain sensor that automatically moves a cap  
48  
49 104 from the dry collector to the wet collector when it rains. Prior to deployment, the buckets were  
50  
51 105 cleaned with a 5% Decon 90 solution and rinsed with ultrapure water (Millipore, Molsheim,  
52  
53 106 France), washed again with 5% HCl solution and finally rinsed again with ultrapure water. After  
54  
55 107 collection, the dry deposition buckets were filled at the laboratory with 500 mL of ultrapure  
56  
57 108 water, and the contents thoroughly leached and filtered. Wet samples were thoroughly leached  
58  
59  
60

1  
2  
3 109 and filtered. The samples were collected on GF/F membranes (0.7  $\mu\text{m}$ , precombusted at 500°C  
4  
5 110 for 6 h before use) and dried at 40°C for 96 h before analysis.  
6  
7

8 111 Hot alkaline hydrolysis was used for free and esterified *p*-coumaric and ferulic acid  
9  
10 112 recovery. The filters (analysed in triplicate) and 250  $\mu\text{L}$  aliquots of internal standard solutions  
11  
12 113 (2.6 and 1.4 mg/L of fully  $^{13}\text{C}$ -labelled ferulic and *p*-coumaric acids, respectively) were placed  
13  
14 114 in methanol (20 mL) with excess  $\text{NaBH}_4$  (70 mg, 30 min at 20°C). This was done to reduce any  
15  
16 115 hydroperoxides in the samples<sup>[15]</sup> that could degrade the phenolic acids during the hot  
17  
18 116 saponification step. Water (15 mL) and KOH (1.7 g) were then added, and the mixture was  
19  
20 117 saponified by refluxing (2 h). After cooling, the contents of the flasks were acidified to pH 1  
21  
22 118 with 2 N HCl and extracted three times with dichloromethane (DCM) (30 mL). The combined  
23  
24 119 DCM extracts were then concentrated by rotary evaporation at 40°C to give the total lipid  
25  
26 120 extract (TLE).  
27  
28  
29  
30  
31  
32

### 33 122 2.3 Derivatisation

34  
35 123 The TLEs were silylated by dissolving them in 100  $\mu\text{L}$  BSTFA and heating at 50°C for 1 h. The  
36  
37 124 mixture was then diluted with ethyl acetate and analysed by mass spectrometric methods.  
38  
39 125 Owing to the high volatility of TMS derivatives of ferulic and *p*-coumaric acids, it is most  
40  
41 126 important to avoid the use of silylation methods that need an evaporation step (as in the case of  
42  
43 127 classical pyridine/BSTFA mixtures).  
44  
45  
46  
47  
48

### 49 129 2.4 Gas chromatography/electron ionization quadrupole time-of-flight mass 50 51 52 130 spectrometry

53  
54 131 Accurate mass measurements were made in full scan mode using an Agilent 7890B/7200  
55  
56 132 GC/QTOF system (Agilent Technologies, Parc Technopolis – ZA Courtaboeuf, Les Ulis,  
57  
58 133 France). A cross-linked 5% phenyl-methylpolysiloxane capillary column (Agilent  
59  
60

1  
2  
3 134 Technologies; HP-5MS Ultra inert, 30 m × 0.25 mm, film thickness 0.25 μm) was used.  
4  
5 135 Analyses were performed with an injector operating in pulsed splitless mode set at 270°C. Oven  
6  
7 136 temperature was ramped from 70°C to 130°C at 20°C min<sup>-1</sup> and then to 300°C at 5°C min<sup>-1</sup>.  
8  
9 137 The pressure of the carrier gas (He) was maintained at 0.69 × 10<sup>5</sup> Pa until the end of the  
10  
11 138 temperature program. Instrument temperatures were 300°C for the transfer line and 230°C for  
12  
13 139 the ion source. The collision gas was nitrogen (1.5 mL min<sup>-1</sup>). Accurate mass spectra were  
14  
15 140 recorded in the range *m/z* 50–700 at 4 GHz with the collision gas opened. The QTOF-MS  
16  
17 141 instrument provided a typical resolution ranging from 8009 to 12252 from *m/z* 68.9955 to  
18  
19 142 501.9706. Perfluorotributylamine (PFTBA) was used for daily MS calibration.  
20  
21  
22  
23  
24 143

## 26 144 2.5 Gas chromatography/electron ionization tandem mass spectrometry

27  
28 145 GC/EIMS and GC/EIMS/MS experiments were conducted using a model 7890A/7010 tandem  
29  
30 146 quadrupole gas chromatography system (Agilent Technologies, Parc Technopolis – ZA  
31  
32 147 Courtaboeuf, Les Ulis, France). A cross-linked 5% phenyl-methylpolysiloxane HP-5MS Ultra  
33  
34 148 inert capillary column (Agilent Technologies; 30 m × 0.25 mm, film thickness 0.25 μm) was  
35  
36 149 used. Analyses were performed with an injector operating in pulsed splitless mode set at 270°C.  
37  
38 150 The oven temperature was ramped from 70°C to 130°C at 20°C min<sup>-1</sup>, then to 250°C at 5°C  
39  
40 151 min<sup>-1</sup> and finally to 300°C at 3°C min<sup>-1</sup>. The pressure of the carrier gas (He) was held at 0.69  
41  
42 152 × 10<sup>5</sup> Pa until the end of the temperature program and then ramped from 0.69 × 10<sup>5</sup> Pa to 1.49  
43  
44 153 × 10<sup>5</sup> Pa at 0.04 × 10<sup>5</sup> Pa min<sup>-1</sup>. The mass spectrometry conditions were: electron energy,  
45  
46 154 70 eV; transfer line temperature, 300°C; source temperature, 230°C; quadrupole 1 temperature,  
47  
48 155 150°C; quadrupole 2 temperature, 150°C; collision gas (N<sub>2</sub>) flow rate, 1.5 mL min<sup>-1</sup> quench  
49  
50 156 gas (He) flow rate, 2.25 mL min<sup>-1</sup>; mass range, *m/z* 50–700; cycle time, 313 ms.  
51  
52 157 Collision-induced dissociation (CID) was optimised by using collision energies of 5, 10, 15 and  
53  
54 158 20 eV.  
55  
56  
57  
58  
59  
60

159

### 3 RESULTS AND DISCUSSION

161

#### 3.1 EIMS fragmentation of *p*-coumaric acid TMS derivative

The TOF mass spectrum of the TMS derivative of *p*-coumaric acid (Figure 1A) displayed a molecular peak at  $m/z$  308.1266 (ions  $\mathbf{a}^{+\bullet}$ ,  $\mathbf{b}^{+\bullet}$  or  $\mathbf{f}^{+\bullet}$ ) and intense peaks at  $m/z$  293.1027, 249.1130 and 219.0835 corresponding to losses of  $\text{CH}_3$ ,  $\text{C}_2\text{H}_3\text{O}_2$  and  $\text{C}_3\text{H}_9\text{OSi}$ , respectively.

The fragmentation pathways in Figure 2 are proposed to explain the formation of these ions.

Ionization of the ester group of the *p*-coumaric acid TMS derivative can take place on the double-bonded oxygen or on the oxygen linked to the TMS group, giving ions  $\mathbf{a}^{+\bullet}$  and  $\mathbf{b}^{+\bullet}$ ,

respectively (Figure 2). Ion  $\mathbf{a}^{+\bullet}$  can easily lose  $\text{TMSO}^\bullet$  to give the ion  $\mathbf{c}^+$  at  $m/z$  219.0835 strongly stabilized by conjugation.<sup>[16]</sup> However, CID analyses (Table 1) showed that this ion

could also be produced from ion  $\mathbf{d}^+$  at  $m/z$  293.1027 resulting from the loss of a methyl radical by the molecular ion  $\mathbf{b}^{+\bullet}$ . This fragmentation should entail the loss of a neutral  $(\text{CH}_3)_2\text{Si}=\text{O}$  by

the fragment ion  $\mathbf{d}^+$  as depicted in Figure 2. This ion can also lose a neutral molecule of  $\text{CO}_2$  as previously proposed by Brook et al.<sup>[17]</sup> in the case of triphenylsilyl benzoates to give the ion  $\mathbf{e}^+$

at  $m/z$  249.1130 also strongly stabilized by conjugation (Figure 2). The shifts of molecular ions ( $\mathbf{a}^{+\bullet}$ ,  $\mathbf{b}^{+\bullet}$  or  $\mathbf{f}^{+\bullet}$ ) and fragment ions  $\mathbf{c}^+$ ,  $\mathbf{d}^+$  and  $\mathbf{e}^+$  to  $m/z$  317.1551  $[\text{M}]^{+\bullet}$ , 228.1142  $[\text{M} - \text{TMSO}]^+$ ,

302.1325  $[\text{M} - \text{CH}_3]^+$  and 257.1391  $[\text{M} - \text{CH}_3 - {}^{13}\text{CO}_2]^+$ , respectively, in TOF MS of fully  $^{13}\text{C}$ -labelled *p*-coumaric acid TMS derivative (Figure 1B) strongly support the proposed

fragmentation pathways. The low deviations (ranging from +2.5 to -0.8 ppm) observed between accurate and calculated masses of ions  $\mathbf{a-e}$  (charges not shown) confirm the elemental

composition of the proposed fragment ions (Table 2).

182

#### 3.2 EIMS fragmentation of ferulic acid TMS derivative

1  
2  
3 184 The TOF mass spectrum of the ferulic acid TMS derivative displayed a molecular peak at  $m/z$   
4  
5 185 338.1371 and intense peaks at  $m/z$  323.1133, 308.0902, 293.0661, 279.1240, 249.0934 and  
6  
7 186 219.0478 (Figure 1C). Fragment ions at  $m/z$  249.0934, 323.1133 and 279.1240 correspond to  
8  
9 187 ions  $\mathbf{c}^+$ ,  $\mathbf{d}^+$  and  $\mathbf{e}^+$ , respectively, whose formation is described above (Figure 2). It was  
10  
11 188 previously demonstrated that compounds possessing a methoxy and a TMS group in the 1,2  
12  
13 189 positions on an aromatic ring can undergo consecutive losses of two methyl radicals to give a  
14  
15 190 stable cyclic radical cation.<sup>[18]</sup> In the case of the molecular ion  $\mathbf{f}^{\bullet}$  of the ferulic acid TMS  
16  
17 191 derivative, this process gives the ion  $\mathbf{h}^{\bullet}$  at  $m/z$  308.0902 (Figure 2), which can then lose another  
18  
19 192 methyl radical to give the stable cation  $\mathbf{i}^+$  at  $m/z$  293.0661.<sup>[19]</sup> Interestingly, ion  $\mathbf{j}^{\bullet}$  resulting  
20  
21 193 from the transfer of the charge of ion  $\mathbf{h}^{\bullet}$  to the ester group can undergo cleavages similar to  
22  
23 194 the molecular ion (i.e. direct loss of  $\text{TMSO}^{\bullet}$  or loss of methyl radical followed by neutral  
24  
25 195  $(\text{CH}_3)_2\text{Si}=\text{O}$  and  $\text{CO}_2$  elimination) to give ions  $\mathbf{l}^+$  and  $\mathbf{m}^+$  at  $m/z$  219.0478 and 249.0762,  
26  
27 196 respectively, (Figure 2). Although the masses of ions  $\mathbf{c}^+$  and  $\mathbf{m}^+$  were too close to be discerned  
28  
29 197 in GC-QTOF analyses,  $^{13}\text{C}$  labelling gave strong support to the proposed fragmentation  
30  
31 198 pathways. The shifts of molecular ions ( $\mathbf{a}^{\bullet}$ ,  $\mathbf{b}^{\bullet}$  or  $\mathbf{f}^{\bullet}$ ) and fragment ions  $\mathbf{d}^+$  or  $\mathbf{g}^+$ ,  $\mathbf{h}^{\bullet}$  or  $\mathbf{j}^{\bullet}$ ,  $\mathbf{i}^+$   
32  
33 199 or  $\mathbf{k}^+$ ,  $\mathbf{e}^+$ ,  $\mathbf{c}^+$ ,  $\mathbf{m}^+$  and  $\mathbf{l}^+$  to  $m/z$  348.1697  $[\text{M}]^{\bullet}$ , 333.1464  $[\text{M} - \text{CH}_3]^+$ , 317.1198  $[\text{M} - \text{CH}_3 -$   
34  
35 200  $^{13}\text{CH}_3]^{\bullet}$ , 302.0980  $[\text{M} - 2\text{CH}_3 - ^{13}\text{CH}_3]^+$ , 288.1528  $[\text{M} - \text{CH}_3 - ^{13}\text{CO}_2]^+$ , 259.1283  $[\text{M} -$   
36  
37 201  $\text{TMSO}]^+$ , 257.1030  $[\text{M} - 2\text{CH}_3 - ^{13}\text{CH}_3 - ^{13}\text{CO}_2]^+$  and 228.0771  $[\text{M} - \text{CH}_3 - ^{13}\text{CH}_3 - \text{TMSO}]^+$ ,  
38  
39 202 respectively, in TOF MS of fully  $^{13}\text{C}$ -labelled ferulic acid TMS derivative (Figure 1D) are in  
40  
41 203 close agreement with these fragmentations. Moreover, CID analyses of  $^{13}\text{C}$ -labelled and  
42  
43 204 unlabelled ferulic acid TMS derivative confirmed the production of ions  $\mathbf{l}^+$  and  $\mathbf{m}^+$  from ion  $\mathbf{j}^{\bullet}$   
44  
45 205 and that of ions  $\mathbf{h}^{\bullet}$  and  $\mathbf{i}^+$  from ion  $\mathbf{g}^+$  (Table 1). The small differences (ranging from +2.9 to  
46  
47 206  $-1.8$  ppm) observed between measured and calculated accurate masses of these different ions  
48  
49 207 (Table 3) also validate the proposed fragmentation mechanisms.  
50  
51  
52  
53  
54  
55  
56  
57  
58  
59  
60

1  
2  
3 208 The driving force for the formation of ions  $\mathbf{c}^+$ ,  $\mathbf{e}^+$ ,  $\mathbf{l}^+$  and  $\mathbf{m}^+$  is their strong stabilization by  
4  
5 209 conjugation with the double bond and the aromatic ring. These fragmentations are thus not  
6  
7  
8 210 specific to TMS derivatives of cinnamic acids but can also be observed in EI mass spectra of  
9  
10 211 TMS derivatives of all benzoic acids (e.g. *p*-hydroxybenzoic and vanillic acids) (Figures 3A  
11  
12 212 and 3B), where the benzylic charge is also highly conjugated with the aromatic ring. By  
13  
14 213 contrast, they are totally lacking in EI mass spectra of TMS derivatives of aromatic acids where  
15  
16 214 this conjugation is not possible, as is the case for the 3-(4-hydroxyphenyl)propanoic acid  
17  
18 215 (phloretic acid) TMS derivative (Figure 3B).  
19  
20  
21  
22 216

### 23 24 217 3.3 MRM quantification of ferulic and *p*-coumaric acid TMS derivatives in 25 26 218 environmental samples

27  
28  
29 219 As an application, the fragmentation pathways described in the previous section were used  
30  
31 220 together with retention times to identify and quantify TMS derivatives of ferulic and *p*-coumaric  
32  
33 221 acids in TLEs of wet- and dry-deposited atmospheric particles collected in the south of France.  
34  
35 222 Silylated TLEs were analyzed in MRM mode using the following specific transitions selected  
36  
37 223 on the basis of the fragmentation pathways described above (Figure 2):  $m/z$  293  $\rightarrow$  219 ( $\mathbf{d}^+ \rightarrow$   
38  
39 224  $\mathbf{c}^+$ ) and  $m/z$  323  $\rightarrow$  279 ( $\mathbf{d}^+ \rightarrow \mathbf{e}^+$ ) for unlabelled *p*-coumaric and ferulic acids, respectively, and  
40  
41 225  $m/z$  302  $\rightarrow$  228 ( $\mathbf{d}^+ \rightarrow \mathbf{c}^+$ ) and  $m/z$  333  $\rightarrow$  288 ( $\mathbf{d}^+ \rightarrow \mathbf{e}^+$ ) for the fully  $^{13}\text{C}$ -labelled corresponding  
42  
43 226 internal standards.  
44  
45  
46

47 227 The limits of detection (10 pg and 30 pg for the TMS derivatives of *p*-coumaric and ferulic  
48  
49 228 acids, respectively) were determined for a signal-to-noise ratio greater than 5. Linear responses  
50  
51 229 with coefficients of determination  $R^2 > 0.99$  could be obtained in the ranges 0.01–1 ng and  
52  
53 230 0.03–3 ng for the TMS derivatives of *p*-coumaric and ferulic acids, respectively.  
54  
55

56 231 Comparison of mass spectral data and retention times with those of standards allowed  
57  
58 232 unambiguous characterization of TMS derivatives of *trans-p*-coumaric and *trans*-ferulic acids  
59  
60

1  
2  
3 233 in all the samples analysed (see example in Figure 4). Large proportions of the *cis* isomers of  
4  
5 234 these compounds could also be detected (Figure 4). The similar isomerization observed in the  
6  
7 235 case of <sup>13</sup>C-labelled internal standards (Figure 5) clearly demonstrates that these *cis* isomers  
8  
9 236 were not present in the samples investigated but were produced during the treatment. This  
10  
11 237 finding is very surprising since alkaline hydrolysis is often used to recover esterified phenolic  
12  
13 238 acid.<sup>[12]</sup> Photoisomerization of hydroxycinnamic acids is well-known <sup>[20]</sup> and it was previously  
14  
15 239 demonstrated that *trans-p*-coumaric and *trans*-ferulic acids underwent *cis* isomerization in  
16  
17 240 methanol during light exposure at ambient temperature.<sup>[21]</sup> However, in the present work,  
18  
19 241 alkaline hydrolyses were carried out in a foil-covered vessel and TLEs were stored in amber  
20  
21 242 vials. Moreover, we note that a marked increase in the proportion of *cis* isomers (up to 80%)  
22  
23 243 could be observed when the alkaline hydrolysis mixture was stored at 4°C for 24 h in the dark.  
24  
25 244 As previously suggested by Istasse et al.<sup>[22]</sup>, light is clearly not the main cause of the  
26  
27 245 isomerisation, which seems instead to be caused by the alkaline conditions used.

28  
29  
30  
31  
32  
33 246 *Cis* and *trans* isomers were summed during the quantification of *p*-coumaric and ferulic  
34  
35 247 acids in the different samples analysed. The results obtained (Table 4), show a high variability,  
36  
37 248 with ferulic acid content ranging from  $13.2 \pm 4$  to  $199.7 \pm 29.7$   $\mu\text{g g}^{-1}$  and *p*-coumaric acid  
38  
39 249 content from  $28.4 \pm 3.5$  to  $895.1 \pm 2.9$   $\mu\text{g g}^{-1}$  in October 2019 and April 2020, respectively.  
40  
41 250 These large differences in values are probably due to the presence of angiosperm/gymnosperm  
42  
43 251 pollens enriched in phenolic compounds during springtime. Pollen grains are released from  
44  
45 252 terrestrial vegetation in large quantities, with different vegetation types delivering pulses into  
46  
47 253 the atmosphere at varying times of the year.<sup>[23]</sup> In the sampling region, production of pollens  
48  
49 254 (dominated by pine, oak, cypress, plane, plantain and grasses)<sup>[24]</sup> runs generally from February  
50  
51 255 to the end of July.<sup>[25]</sup> The presence of pine and oak pollens relatively enriched in *p*-coumaric  
52  
53 256 esters<sup>[26,27]</sup> could explain the very high *p*-coumaric acid/ferulic acid ratios observed in some  
54  
55 257 spring samples (Table 4).  
56  
57  
58  
59  
60

1  
2  
3 2584  
5  
6 259 **4 CONCLUSIONS**

7  
8 260 EIMS fragmentations of *p*-coumaric and ferulic acids were elucidated using low-energy  
9  
10 261 CID-MS/MS, <sup>13</sup>C labelling and accurate mass measurements. Specific MRM transitions based  
11  
12 262 on the fragmentation pathways elucidated were selected and applied to different wet- and dry-  
13  
14 263 deposited atmospheric particle samples collected in the south of France. These transitions  
15  
16 264 proved very useful for identifying and quantifying relatively small amounts of these phenolic  
17  
18 265 acids in complex lipid extracts. We note that a strong *cis*-isomerization of *p*-coumaric and  
19  
20 266 ferulic acid was observed during alkaline hydrolysis of the samples. In any further work to  
21  
22 267 determine the processes responsible for this isomerization, great care should thus be taken when  
23  
24 268 quantifying *cis*- and *trans*-hydroxycinnamic acids in environmental samples involving alkaline  
25  
26 269 treatment.

27  
28  
29  
30  
31 27032  
33 271 **ACKNOWLEDGEMENTS**

34  
35  
36 272 This work was supported by the LEFE-CYBER (Les Enveloppes Fluides et l'Environnement)  
37  
38 273 national program, as part of the ATMOSMER (Etude de la dégradation abiotique des apports  
39  
40 274 ATMOSphériques Sahariens en MER et de leur impact sur la dégradation des communautés  
41  
42 275 phytoplanctoniques marines) research program. Thanks are due to the FEDER OCEANOMED  
43  
44 276 (N° 1166-39417) for the funding of the apparatus used. This work was supported by the  
45  
46 277 National Observation Service MOOSE (Mediterranean Ocean Observing System for the  
47  
48 278 Environment), which helped to provide the atmospheric samples investigated in this study.

49  
50  
51  
52 27953  
54  
55 280 **REFERENCES**

56  
57 281 [1] Kumar N, Pruthi V. Potential applications of ferulic acid from natural sources. *Biotechnol*  
58  
59 282 *Rep.* 2014; 4: 86-93.

- 1  
2  
3 283 [2] Jung HJG, Himmelsbach DS. Isolation and characterization of wheat straw lignin. *J Agric*  
4  
5 284 *Food Chem.* 1989; 37: 81-87.  
6  
7  
8 285 [3] Herring CD, Thorne PG, Lynd LR. *Clostridium thermocellum* releases coumaric acid during  
9  
10 286 degradation of untreated grasses by the action of an unknown enzyme. *Appl Microbiol*  
11  
12 287 *Biotechnol.* 2016; 100: 2907–2915.  
13  
14  
15 288 [4] Multari S, Pihlava JM, Ollenu-Chuasam P, Hietaniemi V, Yang B, Suomela JP.  
16  
17 289 Identification and Quantification of Avenanthramides and Free and Bound Phenolic  
18  
19 290 Acids in Eight Cultivars of Husked Oat (*Avena sativa* L) from Finland. *J. Agric. Food*  
20  
21 291 *Chem.* 2018; 66: 2900–2908.  
22  
23  
24 292 [5] Singh RD, Banerjee J, Arora A. Prebiotic potential of oligosaccharides: A focus on xylan  
25  
26 293 derived oligosaccharides. *Bioact. Carbohydr. Diet. Fibre.* 2015; 5: 19-30.  
27  
28  
29 294 [6] Bei Q, Liu Y, Wang L, Chen G, Wu Z. Improving free, conjugated, and bound phenolic  
30  
31 295 fractions in fermented oats (*Avena sativa* L.) with *Monascus anka* and their antioxidant  
32  
33 296 activity. *J Funct Foods.* 2017; 32: 185-194.  
34  
35  
36 297 [7] Bichot A, Lerosty M, Geinaert L, Médien V, Carrère H, Bernet N, Delgenes JP, Garcia-  
37  
38 298 Bernet D. Soft Microwave Pretreatment to Extract *P*-Hydroxycinnamic Acids from Grass  
39  
40 299 Stalks. *Molecules* 2019; 24: 3885.  
41  
42  
43 300 [8] Buanafina, M. Feruloylation in grasses: current and future perspectives. *Mol. Plant.* 2009;  
44  
45 301 2: 861–872.  
46  
47  
48 302 [9] Minatel IO, Borges CV, Ferreira MI, Gomez HAG, Chen CYO, Lima GPP. Phenolic  
49  
50 303 compounds: functional properties, impact of processing and bioavailability. *Phenolic*  
51  
52 304 *Compd Biol Act.* 2017; 8: 1-24.  
53  
54  
55 305 [10] Rozema J, van de Staij J, Bjorn LO, Caldwell M. UV-B as an environmental factor in  
56  
57 306 plant life: stress and regulation. *Trends Ecol. Evol.* 1997; 12: 22-28.  
58  
59  
60

- 1  
2  
3 307 [11] Proestos C, Sereli D, Komaitis M. Determination of phenolic compounds in aromatic  
4  
5 308 plants by RP-HPLC and GC-MS. *Food Chem.* 2006; 95: 44-52.
- 6  
7 309 [12] Robbins RJ. Phenolic acids in foods: an overview of analytical methodology. *J. Agric.*  
8  
9 310 *Food Chem.* 2003; 51: 2866–2887.
- 10  
11 311 [13] Kumar N, Goel N. Phenolic acids: natural versatile molecules with promising therapeutic  
12  
13 312 applications. *Biotechnol Rep.* 2019; 24: e00370.
- 14  
15 313 [14] Mitani T, Mimura H, Ikeda K, Nishide M, Yamagushi M, Koyama H, Hayashi Y,  
16  
17 314 Sakamoto H. Process for the purification of *cis-p*-coumaric acid by cellulose column  
18  
19 315 chromatography after the treatment of the *trans* isomer with ultraviolet irradiation. *Anal*  
20  
21 316 *Sci.* 2018; 34: 1195-1199.
- 22  
23  
24  
25 317 [15] Galeron MA, Amiraux R, Charriere B, Radakovitch O, Raimbault P, Garcia N, Lagadec  
26  
27 318 V, Vaultier F, Rontani JF. Source and behavior of particulate organic matter in the Rhône  
28  
29 319 River: a lipid approach. *Biogeosciences* 2015; 12: 1431-1446.
- 30  
31  
32  
33 320 [16] Razboršek M, Ivanović M, Kolar M. Validated stability-indicating GC-MS method for  
34  
35 321 characterization of forced degradation products of *trans*-caffeic acid and *trans*-ferulic  
36  
37 322 acid. *Molecules* 2021; 26: 2475.
- 38  
39  
40  
41 323 [17] Brook AG, Harrison AG, Jones PF. Mass-spectral rearrangements of acyloxysilanes and -  
42  
43 324 germanes. *Canadian J Chem.* 1968; 46: 2662-2664.
- 44  
45  
46  
47 325 [18] Horman I, Viani R. Plant-polyphenols and related compounds. A mass-spectrometric study  
48  
49 326 of the trimethylsilyl derivatives of hydroxy- and/or methoxy-substituted cinnamic acids  
50  
51 327 and of their methyl esters. *Org Mass Spectrom.* 1971; 5: 203-219.
- 52  
53  
54  
55  
56  
57  
58  
59  
60

- 1  
2  
3  
4 328 [19] Krauss D, Mainx HG, Tauscher B, Bischof, P. Fragmentation of trimethylsilyl derivatives  
5  
6  
7 329 of 2-alkoxyphenols: a further violation of the 'even-electron Rule'. *Org Mass Spectrom.*  
8  
9  
10 330 1985; 20: 614-618.  
11  
12  
13  
14 331 [20] Katase T. Stereoisomerization of *p*-coumaric and ferulic acids during their incubation in  
15  
16  
17 332 peat soil extract solution by exposure to fluorescent light. *Soil Sci Plant Nutr.* 1981; 17:  
18  
19  
20 333 421-427.  
21  
22  
23  
24 334 [21] Voncina DB, Razboršek M, Simonić M. High performance liquid chromatographic  
25  
26  
27 335 determination of selected phenolic acids in wine. *Nova Biotechnologica* 2009; 9: 113-  
28  
29  
30 336 119.  
31  
32  
33  
34 337 [22] Istasse T, Jacquet M, Berchem T. Extraction of honey polyphenols: method development  
35  
36  
37 338 and evidence of *cis* isomerization ubertas Academica. *Anal Chem Insights* 2016; 11: 49-  
38  
39  
40 339 57.  
41  
42  
43  
44 340 [23] Steiner A, Brooks SD, Deng C, Thornton DCO, Pendleton MW, Bryant V. Pollen as  
45  
46  
47 341 atmospheric cloud condensation nuclei. *Geophys Res Let.* 2015; 42: 3596-3602.  
48  
49  
50  
51 342 [24] Bousquet J, Cour P, Guerin B, Michel FB. Allergy in the Mediterranean area I. Pollen  
52  
53  
54 343 counts and pollinosis of Montpellier. *Clin Allergy* 1984; 14: 249-258.  
55  
56  
57  
58  
59  
60

1  
2  
3  
4 344 [25] Activity report of RNSA (Réseau National de Surveillance Aérobiologique) 2014.

5  
6  
7 345 [www.pollens.fr](http://www.pollens.fr)

8  
9  
10 346 [26] Strohl MJ, Seikel MK. Polyphenols of pine pollen. A survey. *Phytochemistry* 1965; 4:

11  
12  
13 347 383-399.

14  
15  
16 348 [27] Keil RG, Tsamakis E, Giddings JC, Hedges JI. Biochemical distributions (amino acids,

17  
18  
19 349 neutral sugars, and lignin phenols) among size-classes of modern marine sediments from

20  
21  
22 350 the Washington coast. *Geochim Cosmochim Acta* 1998; 62: 1347-1364.  
23  
24  
25  
26  
27  
28  
29  
30  
31  
32  
33  
34  
35  
36  
37  
38  
39  
40  
41  
42  
43  
44  
45  
46  
47  
48  
49  
50  
51  
52  
53  
54  
55  
56  
57  
58  
59  
60

**FIGURE CAPTIONS**

351

352

353 **Figure 1.** TOF mass spectra of TMS derivatives of unlabelled *p*-coumaric (A), fully <sup>13</sup>C-  
354 labelled *p*-coumaric (B), unlabelled ferulic (C), and fully <sup>13</sup>C-labelled ferulic (D) acids.

355

356 **Figure 2.** Proposed fragmentation pathways of TMS derivatives of *p*-coumaric and ferulic  
357 acids.

358

359 **Figure 3.** TOF mass spectra of TMS derivatives of *p*-hydroxybenzoic (A), vanillic (B), and  
360 phloretic (C) acids.

361

362 **Figure 4.** MRM chromatograms ( $m/z$  323 → 279) (A) and ( $m/z$  293 → 219) (B) showing the  
363 presence of *cis*- and *trans*-ferulic and *p*-coumaric acid TMS derivatives, respectively, in the  
364 silylated TLE of wet atmospheric deposits collected on 30 April 2020.

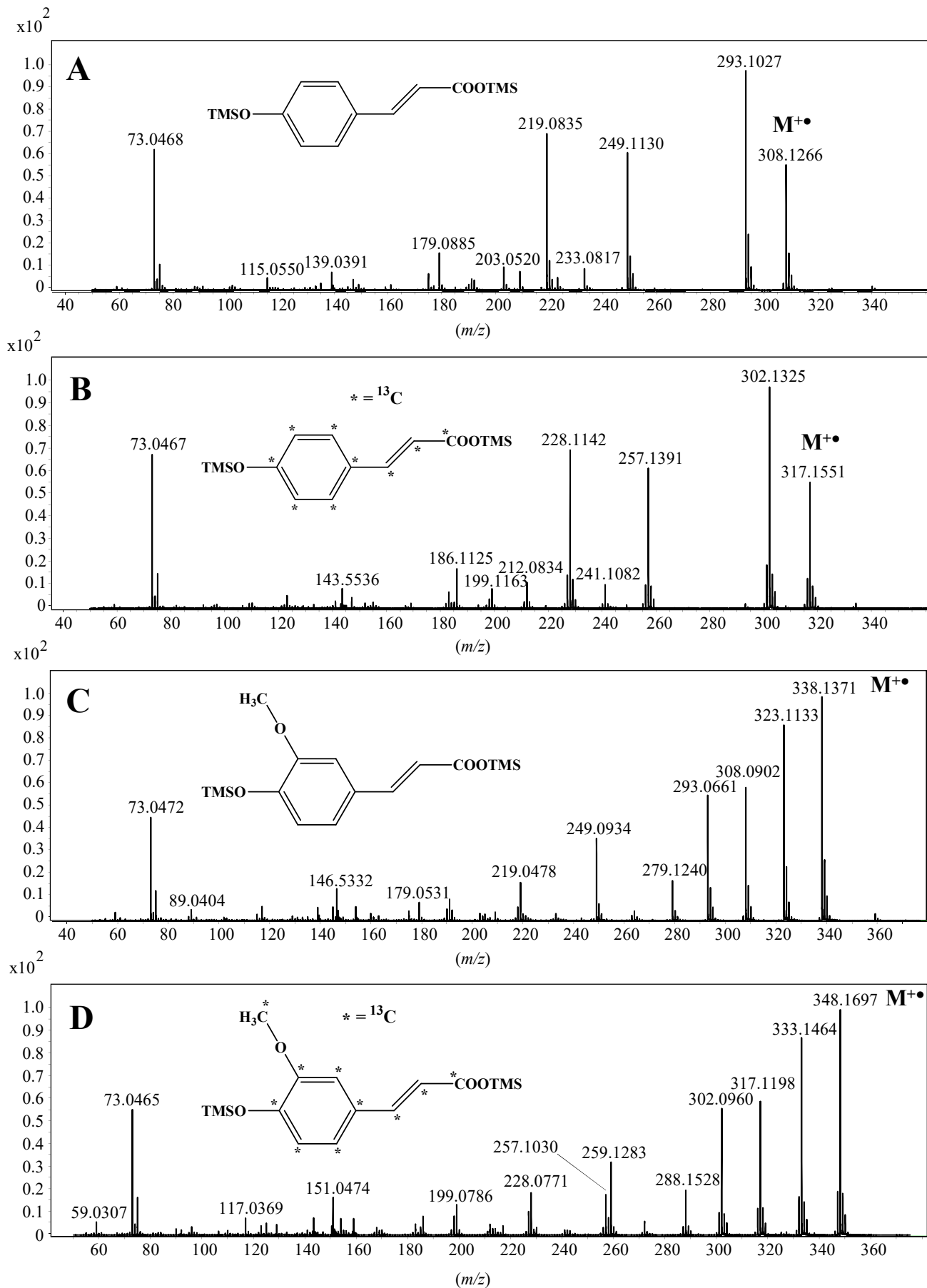
365

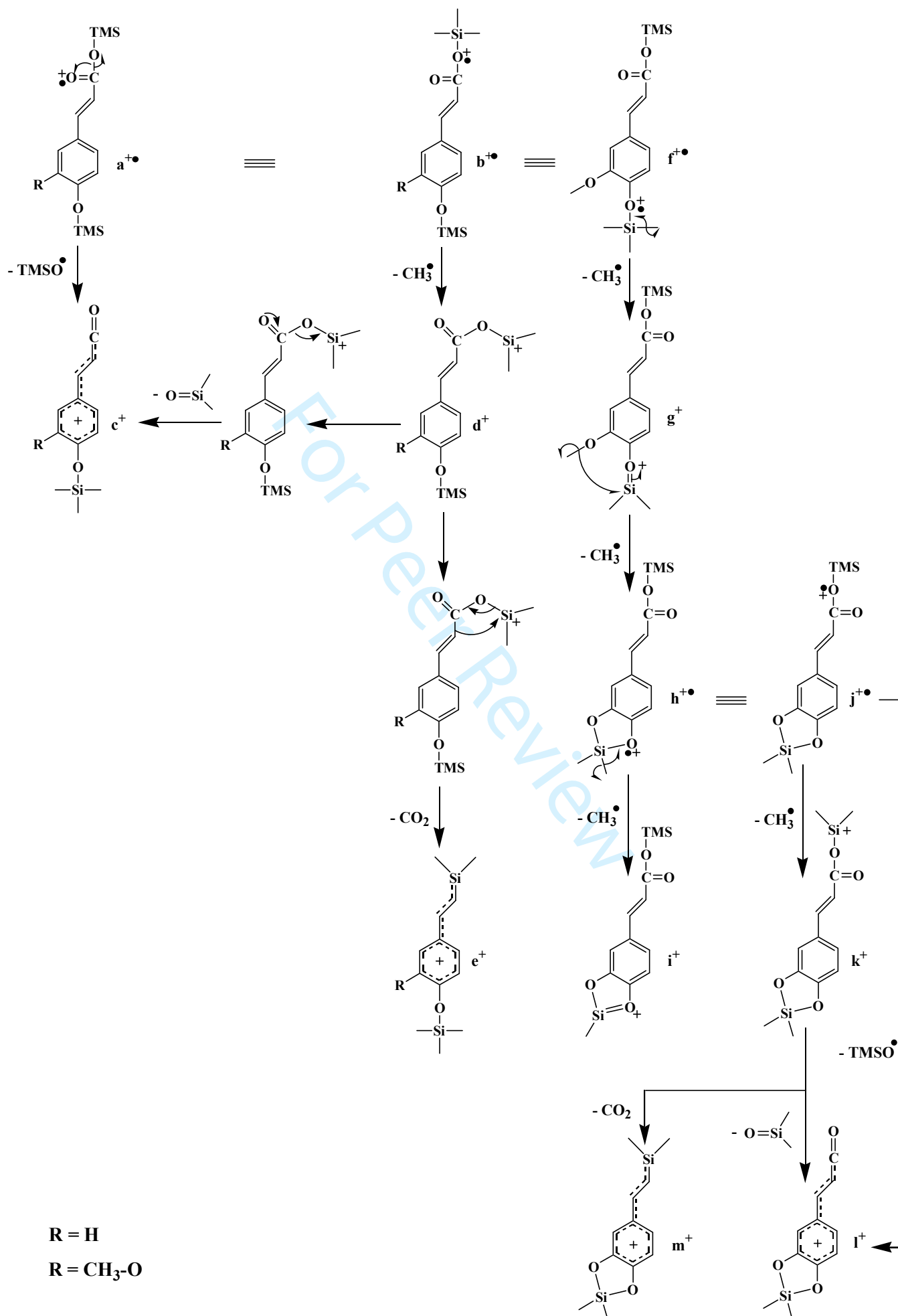
366 **Figure 5.** MRM chromatograms ( $m/z$  333 → 288) of fully <sup>13</sup>C-labelled ferulic acid TMS  
367 derivative before the treatment (A) and after (B).

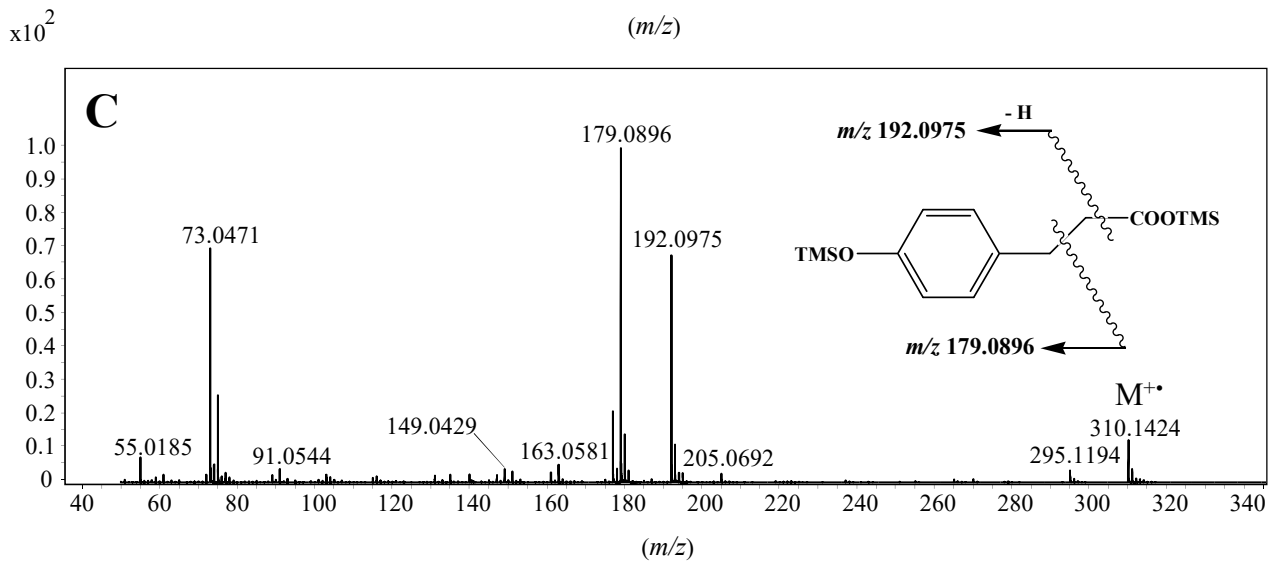
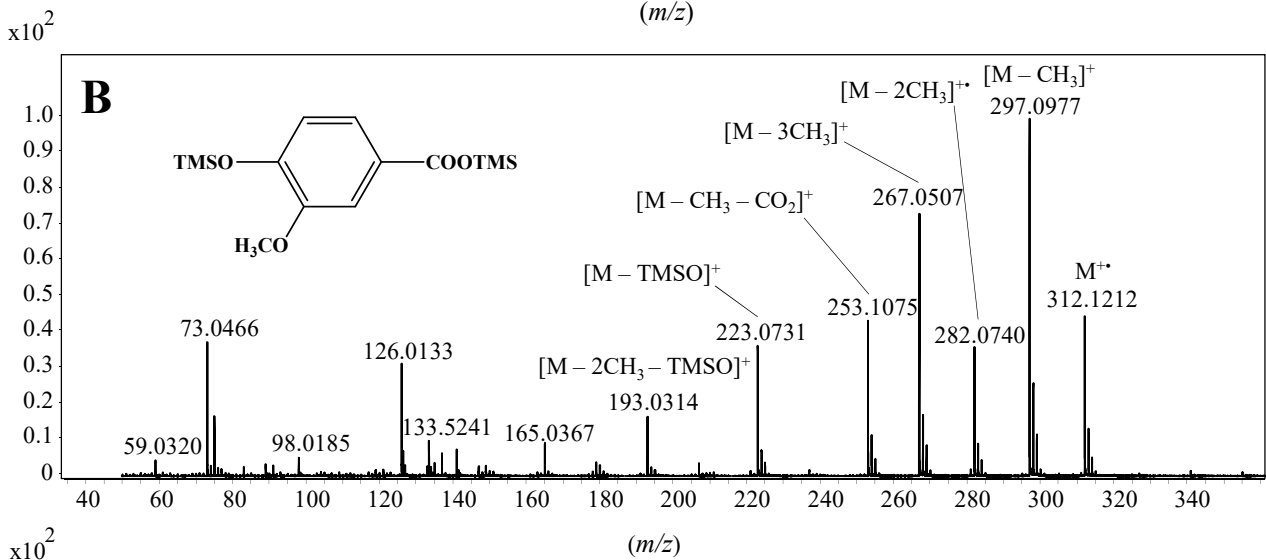
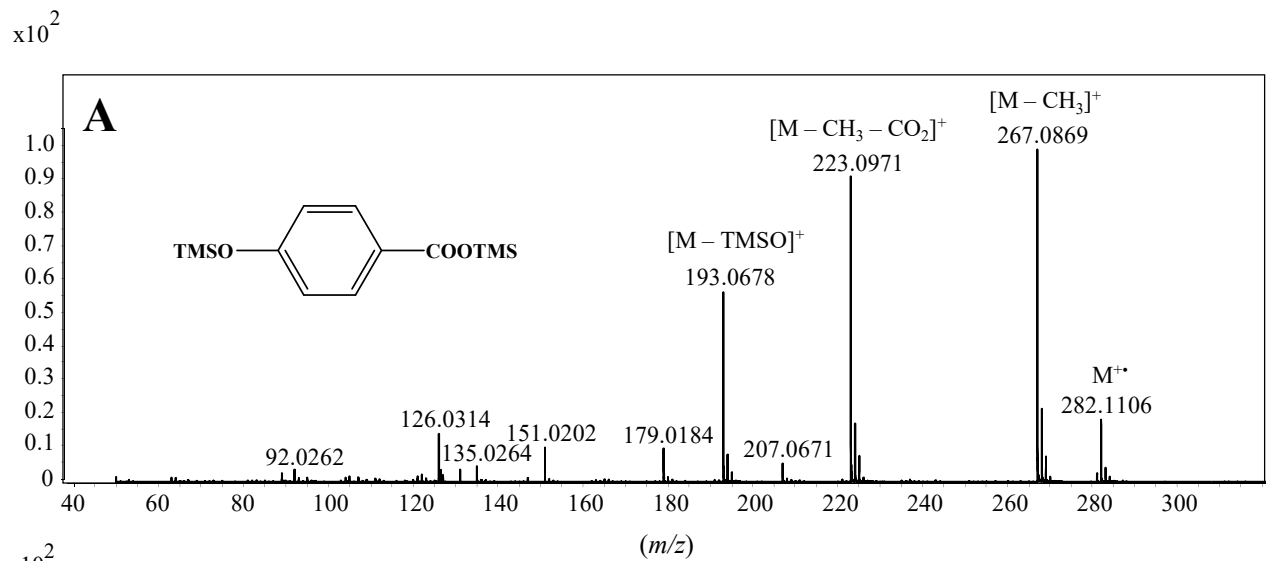
368

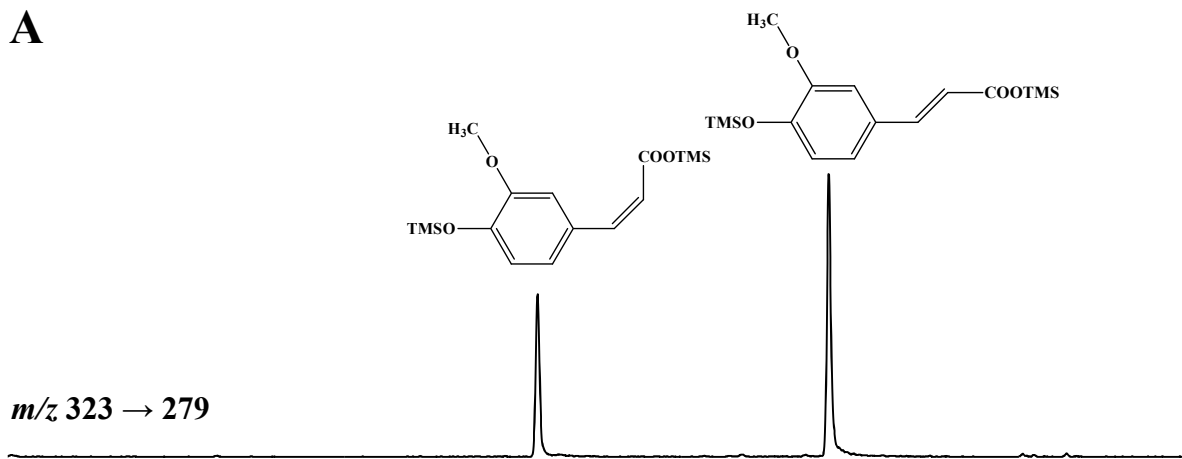
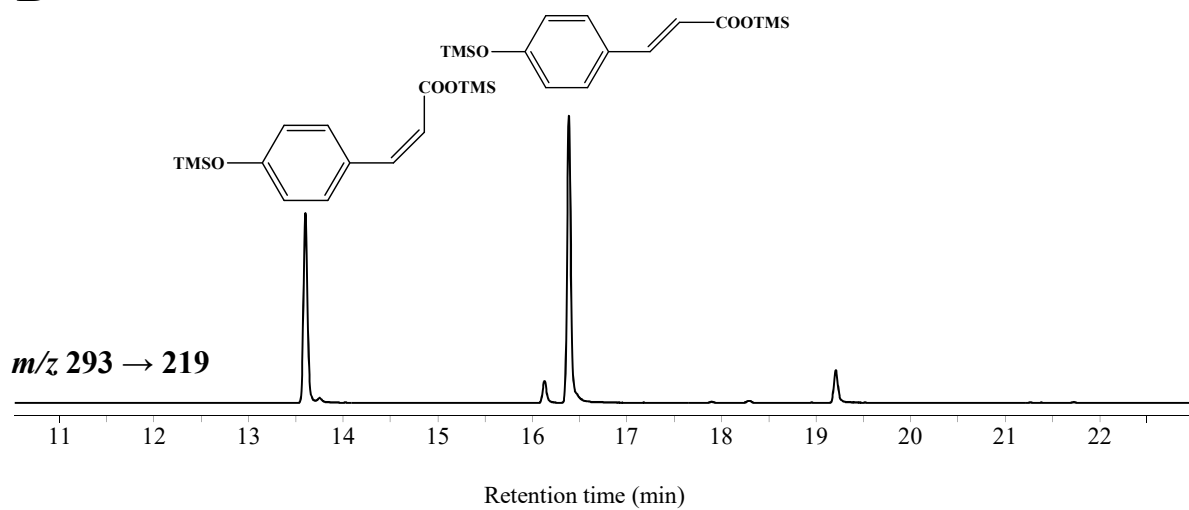
369

370







**A****B**

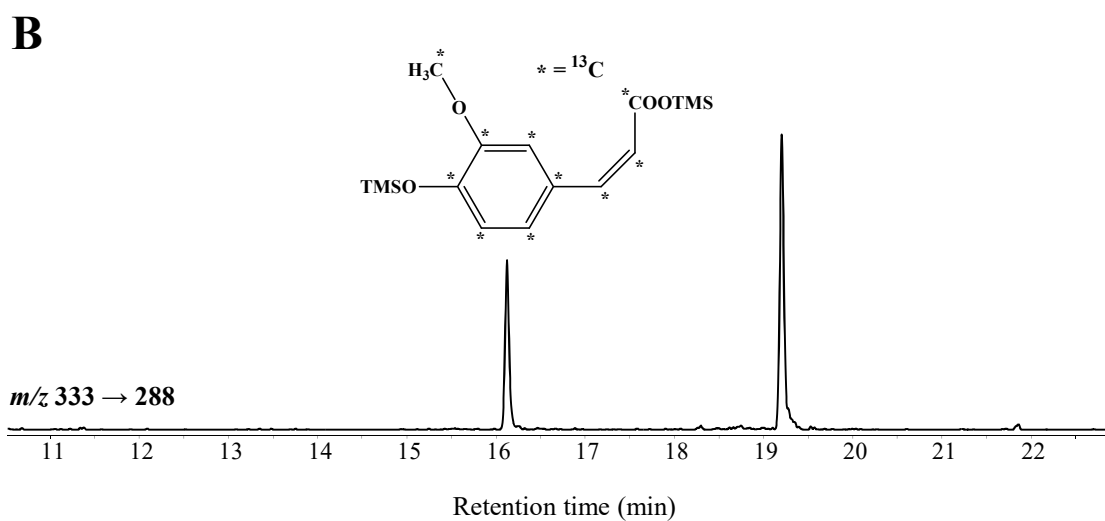
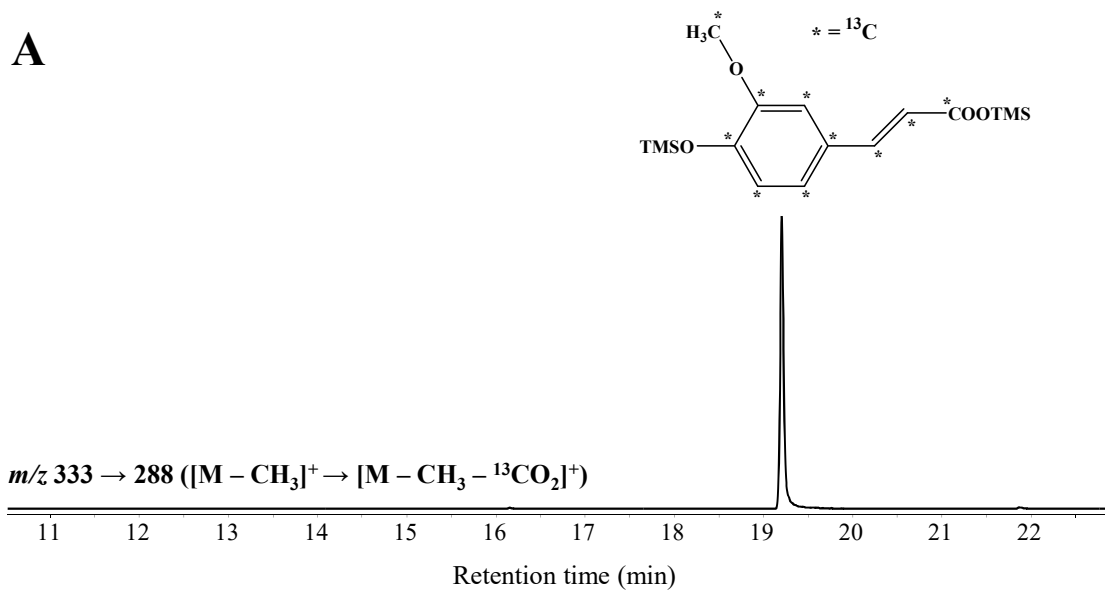


TABLE 1 CID analyses of fragment ions.

Code	<i>m/z</i>	Collision energy (eV)	Product ions
<b>d<sup>+</sup></b>	293 <sup>a</sup>	10	293(49), 249 [- CO <sub>2</sub> ] (79), 233(13), 223(9), 219 [- (CH <sub>3</sub> ) <sub>2</sub> Si=O] (100), 203(6), 73(10)
<b>d<sup>+</sup></b>	302 <sup>b</sup>	10	302(51), 257 [- <sup>13</sup> CO <sub>2</sub> ] (84), 241(13), 229(10), 228 [- (CH <sub>3</sub> ) <sub>2</sub> Si=O] (100), 212(6), 147(5), 73(12)
<b>d<sup>+</sup>, g<sup>+</sup></b>	323 <sup>c</sup>	10	323(61), 308 [- CH <sub>3</sub> ] (72), 293 [-2 CH <sub>3</sub> ] (42), 279 [- CO <sub>2</sub> ] (52), 264(9), 249 [- (CH <sub>3</sub> ) <sub>2</sub> Si=O] (100), 179(8), 175(4), 73(3)
<b>d<sup>+</sup>, g<sup>+</sup></b>	333 <sup>d</sup>	10	333(58), 317 [- <sup>13</sup> CH <sub>3</sub> ] (68), 302 [- <sup>13</sup> CH <sub>3</sub> - CH <sub>3</sub> ] (48), 288 [- <sup>13</sup> CO <sub>2</sub> ] (55), 272(15), 259 [- (CH <sub>3</sub> ) <sub>2</sub> Si=O] (100), 257(16), 186(9), 183(5), 154(3), 73(5)
<b>h<sup>+•</sup>, j<sup>+•</sup></b>	308 <sup>c</sup>	20	308(3), 293 [- CH <sub>3</sub> ] (75), 265(3), 249 [- CH <sub>3</sub> - CO <sub>2</sub> ] (97), 233(9), 219 [- CH <sub>3</sub> - (CH <sub>3</sub> ) <sub>2</sub> Si=O] (100), 192(6), 179(31), 73(3)
<b>h<sup>+•</sup>, j<sup>+•</sup></b>	317 <sup>d</sup>	10	317(3), 302 [- CH <sub>3</sub> ] (75), 257 [- CH <sub>3</sub> - <sup>13</sup> CO <sub>2</sub> ] (98), 241(9), 228 [- CH <sub>3</sub> - (CH <sub>3</sub> ) <sub>2</sub> Si=O] (100), 199(9), 198(5), 186(32), 73(2)

<sup>a</sup> TMS derivative of unlabelled *p*-coumaric acid

<sup>b</sup> TMS derivative of fully <sup>13</sup>C-labelled *p*-coumaric acid

<sup>c</sup> TMS derivative of unlabelled ferulic acid

<sup>d</sup> TMS derivative of fully <sup>13</sup>C-labelled ferulic acid

**TABLE 2** High-accuracy mass spectral data for ions of unlabelled and fully  $^{13}\text{C}$  labelled *p*-coumaric acid TMS derivatives.

Code	Formula	<i>m/z</i> observed	<i>m/z</i> calculated	$\Delta$ (ppm)
<b>a<sup>+•</sup>, b<sup>+•</sup></b>	$^{12}\text{C}_{15}\text{H}_{24}\text{O}_3\text{Si}_2^{+\bullet}$	308.1266	308.1258	+2.6
<b>a<sup>+•</sup>, b<sup>+•</sup></b>	$^{13}\text{C}_9^{12}\text{C}_6\text{H}_{24}\text{O}_3\text{Si}_2^{+\bullet}$	317.1551	317.1550	-0.3
<b>c<sup>+</sup></b>	$^{12}\text{C}_{12}\text{H}_{15}\text{O}_2\text{Si}^+$	219.0835	219.0836	-0.5
<b>c<sup>+</sup></b>	$^{13}\text{C}_9^{12}\text{C}_3\text{H}_{15}\text{O}_2\text{Si}^+$	228.1142	228.1138	-1.0
<b>d<sup>+</sup></b>	$^{12}\text{C}_{14}\text{H}_{21}\text{O}_3\text{Si}_2^+$	293.1027	293.1024	+1.0
<b>d<sup>+</sup></b>	$^{13}\text{C}_9^{12}\text{C}_5\text{H}_{21}\text{O}_3\text{Si}_2^+$	302.1325	302.1326	-0.3
<b>e<sup>+</sup></b>	$^{12}\text{C}_{13}\text{H}_{21}\text{OSi}_2^+$	249.1130	249.1125	+2.0
<b>e<sup>+</sup></b>	$^{13}\text{C}_8^{12}\text{C}_5\text{H}_{21}\text{OSi}_2^+$	257.1391	257.1393	-0.8

**TABLE 3** High-accuracy mass spectral data for ions of unlabelled and fully  $^{13}\text{C}$  labelled ferulic acid TMS derivatives.

Code	Formula	$m/z$ observed	$m/z$ calculated	$\Delta$ (ppm)
<b>a<sup>+•</sup>, b<sup>+•</sup>, f<sup>+•</sup></b>	$^{12}\text{C}_{16}\text{H}_{26}\text{O}_4\text{Si}_2^{+\bullet}$	338.1371	338.1368	+1.8
<b>a<sup>+•</sup>, b<sup>+•</sup>, f<sup>+•</sup></b>	$^{13}\text{C}_{10}\text{C}_6\text{H}_{26}\text{O}_4\text{Si}_2^{+\bullet}$	348.1697	348.1700	-0.9
<b>c<sup>+</sup></b>	$^{12}\text{C}_{13}\text{H}_{17}\text{O}_3\text{Si}^+$	249.0934	249.0941	+2.8
<b>c<sup>+</sup></b>	$^{13}\text{C}_{10}\text{C}_3\text{H}_{17}\text{O}_3\text{Si}^+$	259.1283	259.1278	+1.9
<b>d<sup>+</sup>, g<sup>+</sup></b>	$^{12}\text{C}_{15}\text{H}_{23}\text{O}_4\text{Si}_2^+$	323.1133	323.1130	+0.9
<b>d<sup>+</sup>, g<sup>+</sup></b>	$^{13}\text{C}_{10}\text{C}_5\text{H}_{23}\text{O}_4\text{Si}_2^+$	333.1464	333.1466	-1.0
<b>e<sup>+</sup></b>	$^{12}\text{C}_{14}\text{H}_{23}\text{O}_2\text{Si}_2^+$	279.1240	279.1232	+2.9
<b>e<sup>+</sup></b>	$^{13}\text{C}_9\text{C}_5\text{H}_{23}\text{O}_2\text{Si}_2^+$	288.1528	288.1533	-1.7
<b>h<sup>+•</sup>, j<sup>+•</sup></b>	$^{12}\text{C}_{14}\text{H}_{20}\text{O}_4\text{Si}_2^{+\bullet}$	308.0902	308.0895	+2.3
<b>h<sup>+•</sup>, j<sup>+•</sup></b>	$^{13}\text{C}_9\text{C}_5\text{H}_{20}\text{O}_4\text{Si}_2^{+\bullet}$	317.1198	317.1200	-0.6
<b>i<sup>+</sup>, k<sup>+</sup></b>	$^{12}\text{C}_{13}\text{H}_{17}\text{O}_4\text{Si}_2^+$	293.0661	293.0660	+0.3
<b>i<sup>+</sup>, k<sup>+</sup></b>	$^{13}\text{C}_9\text{C}_4\text{H}_{17}\text{O}_4\text{Si}_2^+$	302.0960	302.0962	-0.7
<b>l<sup>+</sup></b>	$^{12}\text{C}_{11}\text{H}_{11}\text{O}_3\text{Si}^+$	219.0478	219.0472	+2.7
<b>l<sup>+</sup></b>	$^{13}\text{C}_9\text{C}_2\text{H}_{11}\text{O}_3\text{Si}^+$	228.0771	228.0769	+0.9
<b>m<sup>+</sup></b>	$^{13}\text{C}_8\text{C}_4\text{H}_{17}\text{O}_2\text{Si}_2^+$	257.1030	257.1031	-0.4

**TABLE 4** Concentrations and daily mass fluxes of *p*-coumaric and ferulic acids in atmospheric deposits collected in the south of France.

Sampling date (Start-End)	Type of atmospheric deposits	Daily mass fluxes (mg m <sup>-2</sup> d <sup>-1</sup> )	<i>p</i> -coumaric acid (μg g <sup>-1</sup> )	Ferulic acid (μg g <sup>-1</sup> )	Daily <i>p</i> -coumaric acid fluxes (μg m <sup>-2</sup> d <sup>-1</sup> )	Daily ferulic acid fluxes (μg m <sup>-2</sup> d <sup>-1</sup> )	<i>p</i> -Coumaric acid /ferulic acid
21/02/-07/03/2013	Dry	36.37	502.7 ± 2.5	176.4 ± 9.7	18.3 ± 0.1	6.4 ± 0.4	2.86
14/10-31/10/2016	Dry	37.98	78.5 ± 8.6	45.0 ± 15.1	2.9 ± 0.3	1.7 ± 0.6	1.71
24/01-02/02/2017	Wet	28.36	566.7 ± 15.0	149.6 ± 54.3	16.1 ± 0.4	4.2 ± 1.6	3.83
03/02-16/02/2017	Wet	47.36	302.0 ± 54.1	157.4 ± 2.9	14.3 ± 2.6	7.5 ± 1.4	1.91
10/10-24/10/2019	Wet	476.23	28.4 ± 3.5	13.2 ± 4.0	13.5 ± 1.7	6.3 ± 1.9	2.14
12/04-30/04/2020	Wet	65.17	895.1 ± 2.9	199.7 ± 29.7	58.3 ± 0.2	13.0 ± 1.9	4.48
16/01-24/01/2020	Wet	215.13	98.6 ± 17.5	42.6 ± 7.4	21.2 ± 3.8	9.2 ± 1.6	2.30
19/02-24/02/2021	Wet	826.80	80.5 ± 3.6	36.4 ± 6.5	66.6 ± 2.9	30.0 ± 5.4	2.22